Proceedings of the Combustion Institute 40 (2024) 105547

Contents lists available at ScienceDirect

Proceedings of the Combustion Institute

journal homepage: www.elsevier.com/locate/proci

A data-driven, lumped kinetic modeling of OME_{2-5} pyrolysis and oxidation

Timoteo Dinelli [a], Alessandro Pegurri [a], Andrea Bertolino [a,b,c], Alessandro Parente [b,c,d], Tiziano Faravelli [a], Marco Mehl [a], Alessandro Stagni [a,*]

[a] Department of Chemistry, Materials, and Chemical Engineering "G. Natta", Politecnico di Milano, Milano 20133, Italy
[b] Aero-Thermo-Mechanics Laboratory, Université Libre de Bruxelles, Avenue F.D. Roosevelt, Brussels, 1050, Belgium
[c] BRITE - Brussels Institute for Thermal-fluid systems and clean Energy, Brussels, Belgium
[d] WEL Research Institute, Avenue Pasteur, Wavre, 1300, Belgium

ARTICLE INFO

Keywords:
Oxymethylene ethers
Kinetic modeling
Chemical lumping
Rate rules
Optimization

ABSTRACT

The kinetic mechanisms describing the combustion of longer-chain fuels often have limited applicability due to the high number of species involved in their pyrolysis and oxidation paths. In this work, this is addressed for what concerns oxymethylene ethers (OME_n), which recently emerged as synthetic fuel candidates for diesel applications. Starting from an established mechanism representing the pyrolysis and oxidation of dimethoxymethane DMM or OME_1, the combustion chemistry of heavier OMEs up to OME_5 was developed by relying on reaction classes, where structural isomers were lumped into pseudospecies, and the related rates assigned according to analogy and rate rules, considering OME_1 and its lumped chemistry as reference. The obtained lumped model was then coupled to a data-driven optimization methodology, still based on reaction classes, where the consistency among the OME_{2-5} submodules was preserved through scaling factors previously defined. Such a combined approach proved particularly effective in delivering a compact kinetic mechanism, requiring only 48 species on top of the OME_1 model for its extension up to OME_5. The extensive validation and analysis of model predictions show the successful capability of the lumped formulation in representing the chemical behavior of the whole OME family, and the effectiveness of the optimization procedure in further improving model predictions throughout most of the operating space and target properties (ignition delay times in shock tubes, laminar flame speeds, speciations in stirred and flow reactors). The successful implementation of this workflow paves the way for its extensive use for the kinetic modeling of even heavier fuels and its coupling with skeletal reduction techniques to further reduce their size to affordable levels for CFD applications.

1. Introduction

Reaching the ultimate target of a carbon-neutral economy requires an eclectic strategy, such that parallel measures need to be adopted to gradually decrease the dependence on fossil fuels. A crucial drawback of carbon-free, renewable sources like wind or sun is their discontinuous availability, such that storing excess energy and releasing it "on demand" is one of the most coveted goals of the current energy transition. For this reason, the synthesis and use of synthetic fuels, or e-fuels, to accumulate the energy produced from renewable sources has become a major research line [1].

Among e-fuels, oxymethylene ethers (OME_n or $PODE_n$), with recurring molecular structure $CH_3O(CH_2O)_nCH_3$, have been identified as promising alternatives to traditional diesel fuels in internal combustion engines due to various reasons [2]. (i) A reliable catalytic process for their synthesis is nowadays established; (ii) Their physico-chemical properties are similar to those of diesel fuels, especially miscibility and ignition tendencies; (iii) Soot and particulate matter formation are substantially reduced because of their oxygenated nature, as pointed out by a variety of numerical and experimental investigations [3–7].

Consequently, the interest of the scientific community in the chemical kinetics of OMEs has been growing in recent years, in order to characterize its kinetic behavior in terms of reactivity and pollutants formation (e.g. CO and CH_2O, this latter recently being mentioned in the European Union Euro 7 regulation [8]). Most studies have been focusing on dimethoxymethane (DMM or OME_1), which is small enough to perform accurate theoretical calculations of the rate constants and implement them in detailed kinetic models [9–12]. For larger OMEs, the mechanisms are built exploiting analogies with alkanes and smaller ethers, as well as optimization techniques. Reduced mechanisms have also been developed for CFD applications and engine simulations [13–15]. So far, most mechanisms have used OME_3 as a representative fuel molecule, for which the majority of experimental data have been

* Corresponding author.
E-mail address: alessandro.stagni@polimi.it (A. Stagni).

https://doi.org/10.1016/j.proci.2024.105547
Received 4 December 2023; Accepted 25 June 2024
Available online 25 July 2024

collected. Wang et al. [16] and He et al. [17] obtained experimental data and conducted modeling studies on the decomposition in a jet-stirred reactor and the auto-ignition of OME_3. Cai et al. [18] developed a comprehensive mechanism to describe the chemistry of OMEs up to 4. They employed a reaction-class-based approach (with OME_1 [11] as a reference) and leveraged the hierarchy principle to automatically generate reactions and kinetic parameters. Subsequently, they optimized the pre-exponential factors according to reaction rate rules [19] to refine the agreement with the experimental data. Recently, De Ras et al. [20,21] accurately described the oxidation and pyrolysis of OME_2 from theoretical, experimental, and modeling perspectives. Furthermore, Shrestha et al. [22] developed a detailed and comprehensive mechanism up to OME_3 in an ongoing effort to describe the kinetics of OMEs up to 5. The only comprehensive mechanism available up to OME_5, limited to the high-temperature kinetics, was recently done by Kathrotia et al. [23] within a wider modeling effort focused on jet fuel surrogates.

The main issue in developing a comprehensive detailed mechanism for OMEs combustion is the resulting large number of species and reactions, which increases more than linearly with the ethers' length due to the intermediate isomers. Therefore, detailed kinetic models are hardly usable in large-scale calculations, unless prior reduction techniques are employed.

The regular structure of OMEs makes them ideal for a lumped formulation of their kinetics. Previous research [24] demonstrated the effectiveness of the lumping approach in developing mechanisms of long-chain fuels, accurately describing low- and high-temperature chemistry. These methodologies can be combined with an optimization of the kinetic parameters to improve the experimental agreement. Indeed, the compactness of these mechanisms allows them to be quickly optimized against a large database, including different data such as shock tube ignition delay times, speciations in stirred and flow reactors, and even more computationally intensive laminar flame speed calculations.

In this study, we set up a semi-detailed, reaction-class-based formulation of the oxidation and pyrolysis of OMEs up to 5. To the authors' knowledge, this is the first effort implementing such modeling up to OME_5 for both low- and high-temperature, despite its significant presence in commercially available OME blends (as much as ~17 wt% [4]). Subsequently, a data-driven optimization, aimed at preserving coherency among the reaction rates of the different classes was performed to refine model accuracy, by minimizing the dissimilarity between experiments and related predictions. The resulting mechanism was tested against a wide range of experimental conditions and compared with the available state of the art. Finally, conclusions are drawn, and the advantages of the workflow implemented in this work were finally summarized.

2. Methodology

The development of the kinetic model followed a workflow of three sequential steps, respectively: (i) formulation of a core mechanism for the OME_1 as archetypal species of the $OME_{2\text{-}5}$ family; (ii) definition of a kinetic model for $OME_{2\text{-}5}$ pyrolysis and oxidation, based on reaction classes and rate rules; (iii) class-based optimization. Each of these steps is described in detail in the following sections.

2.1. Core mechanism

In the case of OME_1, the limited size of the molecule allows for a detailed description of the elementary steps, based on the large amount of experimental and theoretical literature made available in the latest decade. Following hierarchy and modularity principles, the OME_1 mechanism consists of: (i) a core C_0-C_3 based on the recent updates by Bagheri et al. [25]; (ii) a dimethyl ether (DME or OME_0) chemistry based on the work of Burke et al. [26], updated by Stagni et al. [27]

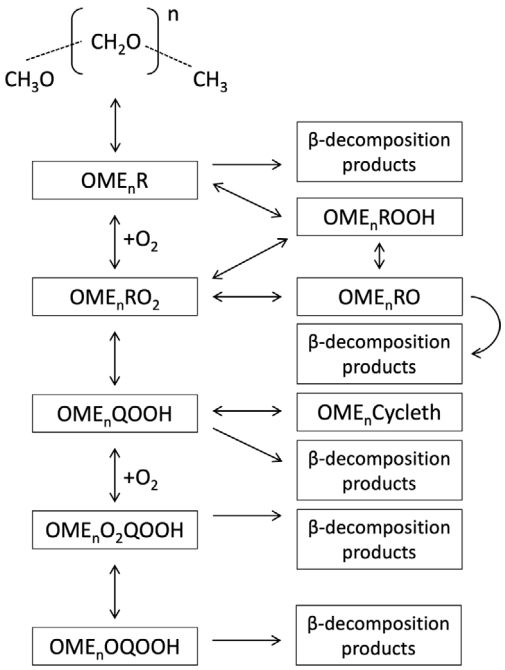

Fig. 1. Lumped oxidation chemistry of OMEs.

for an improved prediction of intermediate species, such as formic and carbonic acid; (iii) a OME_1 sub-mechanism, developed applying a novel methodology [28] that couples chemical lumping to the data-driven optimization of kinetic rates to an established detailed mechanism [11].

In contrast to DME, the longer chain of OME_1 results in the presence of structural isomers among the intermediate species involved in the low- and high-temperature reaction paths, which makes chemical lumping helpful. Reaction classes, which are the starting point of model extension, were identified and classified as described in Section 2.2. For more detail on the OME_1 modeling procedure, the reader is referred to the recent work by Pegurri et al. [28].

2.2. Formulation of $OME_{2\text{-}5}$ model

The sub-mechanism describing the pyrolysis and the oxidation of OMEs longer than OME_1 was built considering it as archetypal for the whole OME family, leveraging its mechanism as formulated in Section 2.1 as a reference. The underlying assumption was that reaction rate constants mostly depend on the reacting moiety of the molecule and the related short-range interactions.

Therefore, it is reasonable to assume that the oxidation chemistry of all OMEs follows the structure reported in Fig. 1, where several similarities can be identified with the oxidation kinetics of *n*-alkanes [24]. Thus, such chemistry can equally benefit from a lumped formulation of the kinetic mechanism. A systematic approach was implemented, based on a reaction class-based methodology, aimed at preserving the self-consistency among the different sub-models. As already done for the reference model of OME_1 [28], reaction classes were defined, and are listed in Table 1. The assignment of first-guess values was performed as follows:

i Unimolecular decomposition pathways (class 1) were updated after the work of Shrestha et al. [22], who performed such an evaluation for OME_2 and OME_3. In analogy, the same decomposition pathways were adopted for $OME_{4\text{-}5}$.

ii The reference values for the H-abstraction reactions (class 2) were derived from our previous work on OME_1 kinetics as detailed in [28]. In such work, the kinetic constants were derived

Table 1
Reaction classes for the high- and low-temperature kinetics of $OME_{2\text{-}5}$.

Reaction class name	ID
Unimolecular decomposition	1
$OME_n + \dot{R}' \leftrightarrow OME_n\dot{R} + R'H$	2
$OME_n\dot{R} \leftrightarrow \beta$-decomposition products	3
$O_2 + OME_n\dot{R} \leftrightarrow OME_nR\dot{O}_2$	4
$R\dot{O}_2 + OME_n\dot{R} \leftrightarrow R\dot{O} + OME_nR\dot{O}$	5
$OME_nR\dot{O}_2 \leftrightarrow OME_n\dot{Q}OOH$	6
$\dot{R} + OME_nROOH \leftrightarrow RH + OME_nR\dot{O}_2$	7
$OME_nROOH \leftrightarrow OME_nR\dot{O} + \dot{O}H$	8
$OME_nR\dot{O} \leftrightarrow \beta$-decomposition products	9
$OME_n\dot{Q}OOH \leftrightarrow OME_n$ cyclic ether	10
$OME_n\dot{Q}OOH \leftrightarrow \beta$-decomposition products	11
$OME_n\dot{Q}OOH + O_2 \leftrightarrow OME_n\dot{O}_2QOOH$	12
$OME_nOQOOH + \dot{O}H \leftrightarrow OME_n\dot{O}_2QOOH$	13
$OME_nOQOOH \leftrightarrow \beta$-decomposition products	14

from the mechanism proposed by Jacobs et al. [11], which underwent lumping and successive optimization. In order to assign these reference values to the kinetic constants of longer-chain OMEs, we applied a framework originally defined for alkanes [24] for the treatment of primary and secondary sites associated with analogous H-atom abstraction sites. As in Ranzi et al. [24], the lumped rate constants were defined based on the number of primary and secondary sites available for H-abstraction, using the equivalent OME_1 H-abstraction rates as reference values.

iii Similarly to what was done for the H-abstraction (class 2), the β-decomposition (classes 3,8,10,13,14) reactions, have a kinetic constant derived from our previous kinetic study [28]. The kinetic parameters are then extrapolated to heavier OMEs in a manner consistent with the methodology employed in the reference studies [24,29].

iv The remaining classes (4, 5, 6, 7, 9, 11, 12) are represented by a single rate in the lumped OME_1 mechanism. Consequently, a single rate constant, derived from the OME_1 mechanism, was assigned to each class. The extrapolation to heavy OMEs was made with the same value as OME_1 as a first estimate.

In this procedure, all the reactions affected by equilibrium (e.g. $OME_nR\dot{O}_2$ isomerization to OME_nQOOH) were written as irreversible in both directions, due to the fictitious nature of the pseudo-species, as always done for lumped mechanisms [30].

This procedure resulted in a lumped mechanism describing the whole $OME_{2\text{-}5}$ chemistry, involving 183 species and 2532 reactions. As expected, such an approach allowed a linear increase in the number of species, contrary to the stronger increase observed for the detailed mechanism due to the larger number of structural isomers to be represented. Starting from the OME_1 mechanism (136 species), the integration of the lumped sub-mechanism required 48 species up to n = 5. Fig. 2 compares the increase in the mechanism size with the OME chain length, against detailed literature approaches [18,22], and confirms an escalating advantage with increasing OME size.

2.3. Optimization

The obtained mechanism underwent an optimization procedure based on reaction classes in the context of the OptiSMOKE++ framework [31]. OptiSMOKE++ implements heuristic optimization strategies to iteratively calibrate kinetic parameters, to refine the agreement with target experiments (e.g. measurements in ideal reactors and 1D laminar flames [32]), as well as artificially generated data [28]. It adopts the OpenSMOKE++ libraries [33] for the ideal reactor modeling as well as the management of detailed kinetics while exploiting the DAKOTA toolkit for the optimization part. Regarding the objective function, OptiSMOKE++ adopts the CurveMatching framework [34,35]

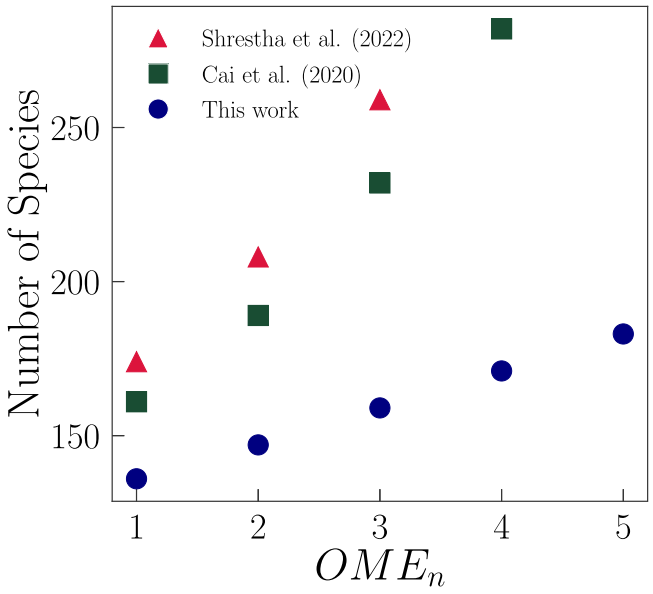

Fig. 2. Total Number of Species included in the kinetic mechanism with respect to the growing length of the OME, compared against available models [18,22].

to quantify the difference between experimental datasets and model predictions, based on the concept of curve similarity. Four sets of independent indices were defined, bounded between 0 and 1, including an extended L^2-norm and Pearson correlations, to compare curve shapes and their first derivatives. Thus, the performance of the model can be summarized by the average of the four indices as reported in Eq. (1).

$$CM_{score} = \frac{d^0_{L^2} + d^1_{L^2} + d^0_{Pe} + d^1_{Pe}}{4} \tag{1}$$

where the subscripts L^2 and Pe respectively refer to L^2-norm and Pearson correlation, and the superscripts 0 and 1 refer to the curves and their first derivatives (their detailed evaluation is available in [34]).

To incorporate the uncertainty of each experimental measurement, a bootstrapping procedure [34] was implemented in OptiSMOKE++ and included in the objective function. As a result, the value of each model-experiment comparison, as defined in Eq. (1), also provides information on the statistical error due to experimental uncertainty. Such a procedure has been successfully applied in previous works [32].

The objective function, accounting for experimental uncertainty, is presented in Eq. (2):

$$Obj = \frac{1}{N}\sum_{i}^{N}\left(1 - \frac{1}{N_b}\sum_{j}^{N_b} CM_{i,j}\right) \tag{2}$$

The modified Arrhenius expression, written in the logarithmic form, is adopted as proposed by Fürst et al. [31] and reported in Eq. (3) to treat all selected rate constant parameters:

$$\mathcal{K} = ln(k) = ln(A) + \beta ln(T) - \frac{E_a}{RT} \tag{3}$$

Therefore, an uncertainty factor (f_r) is assigned to each rate, as discussed in Section 3.1 in the form defined in Eq. (4):

$$f_r = \frac{\mathcal{K}_{max} - \mathcal{K}_0}{ln(10)} = \frac{\mathcal{K}_0 - \mathcal{K}_{min}}{ln(10)} \tag{4}$$

The parameters to be optimized are the pre-exponential factor A, the temperature exponent β, and the activation energy E_a. They were considered as continuous random variables, assumed to have a normal distribution. Additionally, they underwent non-linear constraints derived from Eq. (4) during the optimization process: if the obtained sets of Arrhenius parameters violated these constraints, they were excluded by applying a penalty function.

Based on the concept that all reactions within a given reaction class share a common reference parameter, the mechanism was built by applying analogy rules and assigning the kinetic parameters by consistently scaling the three Arrhenius parameters, according to the rules listed in Section 2.2. The approach then optimizes these parameters for the reference kinetics and, while keeping the scaling factors, scales all reactions belonging to the same class according to the following rules:

$$ln(A) = f^{A}_{scaling} \times ln(A_{ref}) \tag{5}$$

$$\beta = f^{\beta}_{scaling} + \beta_{ref} \tag{6}$$

$$\frac{E_a}{R} = f^{\frac{E_a}{R}}_{scaling} + \left(\frac{E_a}{R}\right)_{ref} \tag{7}$$

where $f^{A}_{scaling}$, $f^{\beta}_{scaling}$ and $f^{\frac{E_a}{R}}_{scaling}$ correspond to the original ratio (for the first one) and difference (for the other two) between the reference kinetic parameters ($ln(A_{ref})$, β_{ref} and $\left(\frac{E_a}{R}\right)_{ref}$) and the ones considered. As a result, the proportion was kept between the reference kinetic parameters and the parameters of the reactions involving heavier OMEs. It is crucial to recognize that while this procedure enforces a set of physical rules, it also introduces implicit additional constraints, which in turn affect the optimization results.

3. Results and discussion

3.1. Selection of optimization targets

The selection of the reactions to be optimized was made by a systematic calculation of the local, normalized sensitivity coefficients over the whole range of operating conditions and according to the reactor type. For the ignition delay times, sensitivities to the CH and OH mass fractions were calculated at the inflection point of each ignition curve. Sensitivity analyses on reactants were performed on the JSR experimental measurements, at temperatures corresponding to the onset of the fuel conversion (~5%). As a result, 11 classes of reactions were identified for optimization. For each of them, a conservative uncertainty factor f_r equal to 0.3 up to 0.5 was assumed. This corresponds to a maximum variation of the optimized rate constants of a factor ~2-3 with respect to the original values.

The experimental datasets adopted for the optimization were selected from the whole database collected from the available literature, which is reported in the Supplementary Material (SM). The target used for optimization was selected, among the Jet Stirred Reactor and Ignition Delay Time measurements, to be representative of the experimental conditions, covering the whole Temperature, Pressure, and Composition space. Specifically, the optimization was conducted using five sets of ignition delay times and five sets of jet stirred reactor measurements. No measurements for the OME_5 were employed during the optimization to adhere to the standard train–test split methodologies. This was done for validation purposes, as well, given that the only dataset available for these fuels in a flow reactor setup is that of Gaiser et al. [7].

3.2. Model validation

The optimized mechanism underwent a wide-range validation involving $OME_{2\text{-}5}$, using the available experimental datasets from shock tubes, laminar flame speeds, and speciation in jet-stirred and flow reactors. The entire set of comparisons was performed leveraging the automatic validation features of SciExpeM as detailed in the following works [37,38], and results of the validation are reported in the supplementary material.

Following a hierarchic methodology, pyrolysis was first validated against the available data. Fig. 3 compares the experimental mole fraction profiles of $OME_{2\text{-}3}$ pyrolysis, as obtained in a jet-stirred reactor

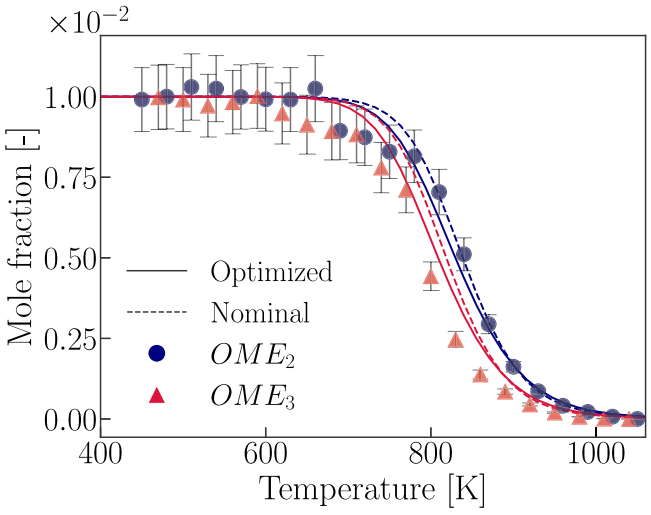

Fig. 3. OME_2 and OME_3 pyrolysis with Ar as a bath gas in a jet-stirred reactor at 1 atm, $\tau = 2\ s$. Symbols: experimental data from Zhong et al. [36].

at 1 atm and 400 K ≤ T ≤ 1000 K by Zhong et al. [36]. The related predictions are reported, including those from both the optimized and nominal (originally lumped) models.

It is possible to observe that the semi-detailed model is already successful in predicting OME decomposition. The relative reactivity is satisfactorily predicted, too, and the model can reproduce the anticipated onset of OME_3. Despite that, the optimization process resulted in a further improvement of the OME_2 and OME_3 profile, while OME_3 predictions were still within the experimental uncertainty.

Fig. 4 compares the capability of the nominal and optimized mechanisms in predicting the IDTs of $OME_{2\text{-}4}$/air stoichiometric mixtures, at P = 10–20 bar, as measured by Cai et al. [18]. The nominal mechanism reasonably predicts the ignition behavior in all cases, with the best performance achieved for OME_2.

The optimization of the nominal model resulted in a significant improvement for both OME_3 and OME_4 in terms of agreement with the experimental measurements. In general, the predictions of the optimized model are very good at 20 bar for all OMEs, while the major discrepancies can be observed at 10 bar in the high-temperature region for OME_3. However, the most remarkable highlight in this comparison is the coherent scaling of reactivity between the different OMEs: regardless of the experimental data, their predictions with the optimized model share a decreased reactivity at the lower temperatures and a slightly increased one at the highest temperature, compared to the nominal mechanism. This underlines the effectiveness of the rate-rule-based optimization methodology in maintaining the physical consistency of the mechanism.

To corroborate this, Fig. 5 analyzes the variation in the kinetic rates for $OME_{2\text{-}4}$ at Φ = 1.0, P = 20 bar, and T = 785 K for the 10 most sensitive reactions. Here, OH mass fraction was considered as representative of IDT, and sensitivity values were sampled at the time of the first ignition delay.

For each reaction, the ratio between the nominal and the optimized kinetic rates is reported. The very good qualitative agreement between every triplet of sensitivity values confirms the coherency of the different sub-models. This holds for all the reaction classes, including the β-decompositions of the $OME_{2\text{-}4}$OQOOH radicals, returning respectively the radicals OCH_2OCHO, CH_3O, and OCHO with different co-products due to the variable chain length.

The validity of the proposed approach is further confirmed by looking at the variation between optimized and nominal rates: the reverse rate of OME_nQOOH oxidation to OME_nO_2QOOH, slowing down ignition, was indeed increased, while the β-decompositions of

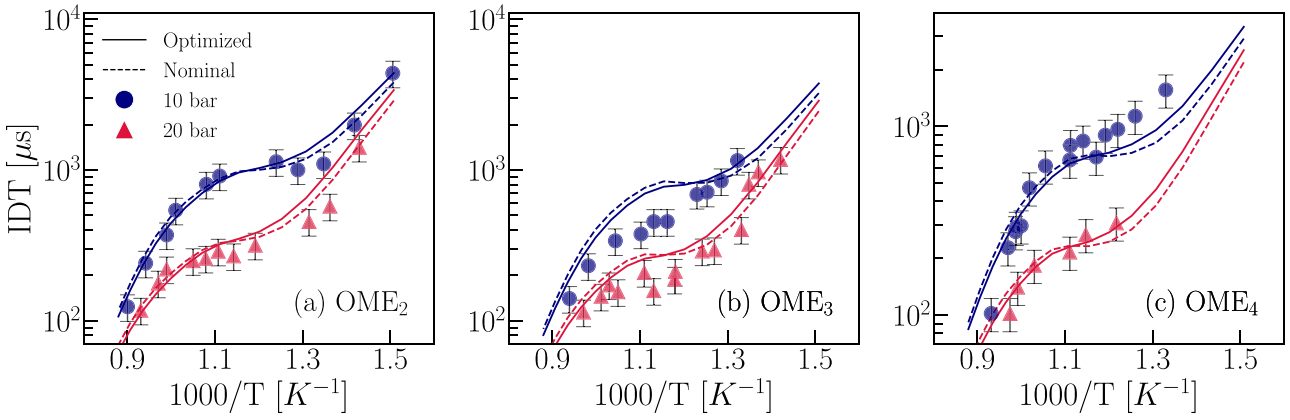

Fig. 4. $OME_{2\text{-}4}$-air ignition delay time in shock tube at $\phi = 1$. Experimental measurements from Cai et al. [18].

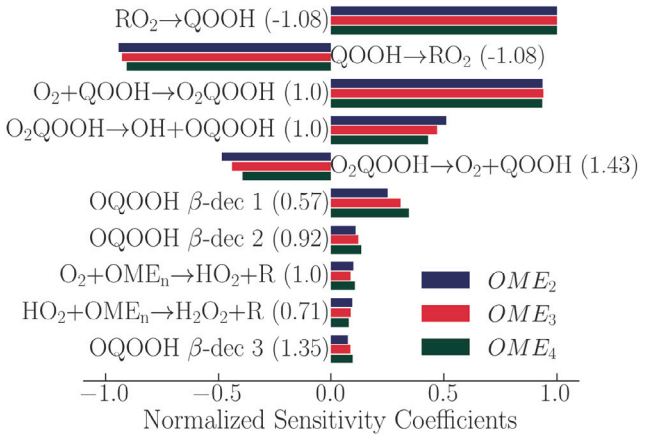

Fig. 5. Normalized sensitivity coefficients of the 10 most sensitive reactions for OH mass fraction in OMEs autoignition. $\Phi = 1.0$, $P = 20$ bar, and $T = 785$ K. For each reaction, the coefficients for $OME_{2\text{-}4}$ are reported. Values in brackets represent the ratio between optimized and original rates at $T = 785$ K (identical for all OMEs).

OME_nOQOOH providing OCH_2OCHO and CH_3O, enhancing ignition, were decreased. The same holds for the H-abstraction by HO_2. On the other hand, the reverse isomerization $OME_nQOOH \rightarrow OME_nRO_2$ was coherently (slightly) decreased. The increase in OME_nRO_2 isomerization, and the third β-decomposition providing OCHO could sound counterintuitive at first glance, but it must be considered that the optimization database extended well beyond the dataset shown in Fig. 4, and that (i) the acceleration in OME_nRO_2 isomerization was anyway minor (less than 10%), and that (ii) the sensitivity coefficient of the mentioned β-decomposition was the lowest one among those shown in Fig. 5. Overall, the sensitivity chart reflects the general slowdown of the reactivity after optimization and is coherent with the higher reactivity of the nominal model.

The general validity of the proposed mechanism is confirmed by the model predictions for laminar flame velocity measurements, laminar flame speciation measurements, and plug flow reactor measurements. SM reports the full benchmark of the final model against them. It is worth highlighting that these experiments were not included in the optimization, but were rather used as validation sets. Moreover, with regard to laminar flame speed, only minor improvements are expected to be obtained by the optimization of OME_n chemistry, as their value is mostly determined by C_0-C_3 chemistry [39], whose rates were not modified in this work to retain the consistency and generality features of the mechanism.

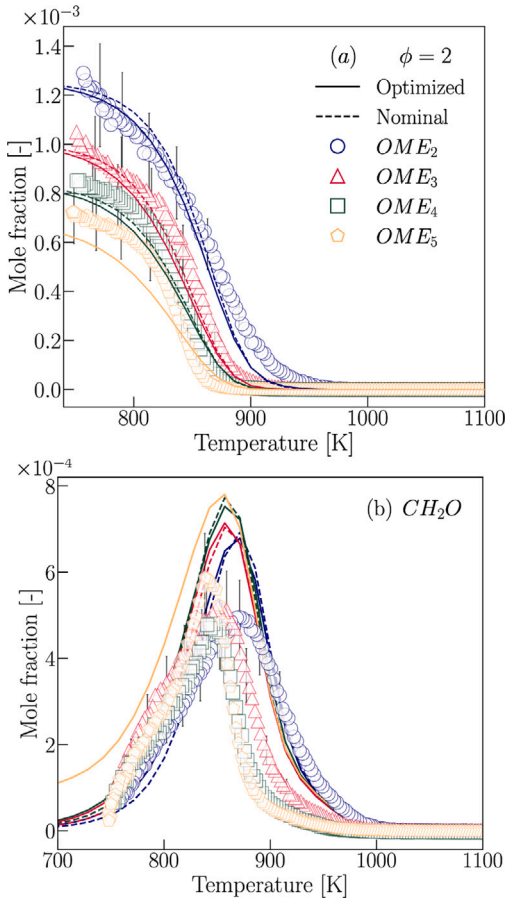

Fig. 6. Oxidation of $OME_{2\text{-}5}/O_2/Ar$ in a flow reactor at $\phi = 2$, 1 atm and $\tau = 1.7$–2.8 s. Symbols are experimental measurements from Gaiser et al. [7] of (a) fuel decomposition and (b) formaldehyde formation.

The mechanism validation was also extended to OME_5. To the authors' knowledge, no experimental data are available concerning its ignition behavior and speciation in jet-stirred reactors. Thus, it was not part of the optimization. The only experimental measurements found in the literature involve its speciation in a flow reactor, as obtained by Gaiser et al. [7]. Still, according to the authors' latest knowledge, these data for $OME_{2\text{-}5}$ are the only ones reported in the literature under flow reactor conditions (jet-stirred measurements are reported in the SM).

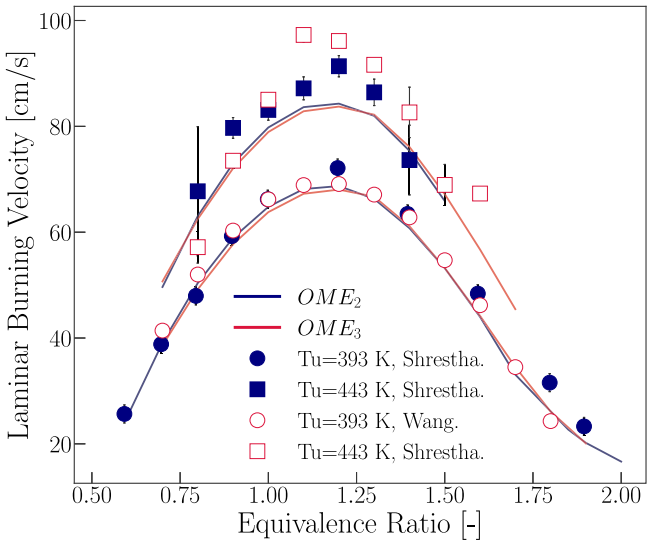

Fig. 7. Laminar flame speed measurements of OME_2 and OME_3. Symbols are experimental data from Shrestha et al. [22] and Wang et al. [40]. Lines are simulations with the nominal model.

Fig. 6(a) shows the related data, concerning the oxidation of $OME_{2\text{-}5}/O_2/Ar$ at $\phi = 2$. Both models exhibit reasonable prediction features in terms of the onset of the fuel decomposition. Considering the experimental uncertainty reported in the study (between 15 and 20%, for species using direct calibration), predictions are always within the uncertainty bars for all OMEs except for OME_5 in the temperature range $800\ K \leq T \leq 900\ K$. Fig. 6(b) depicts the measured CH_2O resulting from the $OME_{2\text{-}5}$ consumption. Even for such an intermediate species, the model predictions are reasonable and coherent with the experimental data, and justify the use of the model in a context where the regulations of CH_2O are being gradually introduced [8].

As a last assessment of the mechanism predictivity features, Fig. 7 compares the experimental laminar flame speeds of OME_2 and OME_3 at the same unburned gas conditions with model predictions. The comparisons highlight both the coherency between experimental data and the consistency of modeling predictions between the different OMEs. Except at $T = 443$ K, with $1.1 \leq \Phi \leq 1.4$, where measurements are in disagreement, OME_2 and OME_3 show very similar laminar flame velocities, also keeping into account the experimental uncertainty. Comparably, modeling predictions are nearly identical for OME_2 and OME_3, as a confirmation that the shared core chemistry drives flame propagation. However, from the available literature data, fully shown in the SM, an agreement between the experimental measurements in different facilities and comparable conditions is not always established: in the near future, more systematic experimental investigations for the different fuels, using comparable facilities, will provide at least qualitative guidelines for model improvements.

4. Conclusions

In this work, the kinetic modeling of oxymethylene ethers up to OME_5 was performed hierarchically with a novel methodology based on the coupling between the systematic construction of a semi-detailed mechanism employing reaction classes and rate rules, and a data-driven optimization for the refinement of the reaction rates of the different classes. For this purpose, a hierarchically-lumped mechanism was developed in a modular way, starting from a consolidated C_0-C_3 core mechanism, then adding literature sub-mechanisms for dimethyl ether (DME) and dimethoxymethane (DMM or OME_1). OME_1 was leveraged as the archetypal species to systematically extend its mechanism up to OME_5, for the first time in the available literature, to the authors' knowledge. Lumping the structural isomers into pseudospecies allowed a linear increase in the number of species with the number of oxymethylene groups, with an increasing advantage with the OME size.

Subsequently, the lumped mechanism underwent an optimization procedure based on reaction rate rules, taking into account a wide range of experimental data, fuels, and operating conditions. The use of scaling factors for all of the three Arrhenius parameters of each reaction rate made it possible to retain the consistency and the physical meaning of the different reaction classes among the different OMEs. The obtained mechanism was finally validated in a wide range of operating conditions: its full benchmark confirmed its predictive features for the whole OME family, underscoring the broad value and competitiveness of semi-detailed approaches for the kinetic modeling of pyrolysis and oxidation processes.

Novelty and Significance Statement

To the authors' knowledge, this is the first work in literature proposing a comprehensive lumped mechanism describing the low- and high-temperature chemistry of oxymethylene ethers (OMEs) up to OME5. The existing low-to-high temperature mechanisms identified in the literature are, in fact, representative of OMEs up to OME4. Moreover, in terms of the size of the mechanisms, they include an elevated number of species due to their detailed formulation. Thus, this work can be considered novel in two directions: it includes the full palette of OME2-5, essential to describe the variable composition of the related fuel mixtures, and its semi-detailed formulation eases its use from a computational point of view, as a reduced number of species is needed, with satisfactory performance in the whole range of operating conditions. Its significance is also extended to the delivered mechanism, in the standardized CHEMKIN format, made available to the kinetic and fluid-dynamic community, to enhance further research activity in this field.

CRediT authorship contribution statement

Timoteo Dinelli: Designed methodology, Performed research, Wrote the paper. **Alessandro Pegurri:** Provided kinetic expertise, Wrote the paper. **Andrea Bertolino:** Provided numeric expertise, Revised the paper. **Alessandro Parente:** Supervised methodology definition, Revised the paper. **Tiziano Faravelli:** Methodology definition, Revised the paper. **Marco Mehl:** Provided kinetic expertise, Revised the paper. **Alessandro Stagni:** Designed and supervised methodology definition, Revised the paper.

Declaration of competing interest

The authors declare that they have no known competing financial interests or personal relationships that could have appeared to influence the work reported in this paper.

Appendix A. Supplementary data

Supplementary material is provided with the paper.

Supplementary material related to this article can be found online at https://doi.org/10.1016/j.proci.2024.105547.

References

[1] A. Ramirez, S.M. Sarathy, J. Gascon, CO2 derived E-Fuels: Research trends, misconceptions, and future directions, Trends Chem. 2 (9) (2020) 785–795.
[2] K. Kohse-Höinghaus, Combustion in the future: The importance of chemistry, Proc. Combust. Inst. 38 (1) (2021) 1–56.
[3] J. Liu, H. Wang, Y. Li, Z. Zheng, Z. Xue, H. Shang, M. Yao, Effects of diesel/PODE (polyoxymethylene dimethyl ethers) blends on combustion and emission characteristics in a heavy duty diesel engine, Fuel 177 (2016) 206–216.

[4] A. Omari, B. Heuser, S. Pischinger, C. Rüdinger, Potential of long-chain oxymethylene ether and oxymethylene ether-diesel blends for ultra-low emission engines, Appl. Energy 239 (2019) 1242–1249.

[5] F. Ferraro, C. Russo, R. Schmitz, C. Hasse, M. Sirignano, Experimental and numerical study on the effect of oxymethylene ether-3 (OME3) on soot particle formation, Fuel 286 (2021) 119353.

[6] R. Schmitz, C. Russo, F. Ferraro, B. Apicella, C. Hasse, M. Sirignano, Effect of oxymethylene ether-2-3-4 (OME2-4) on soot particle formation and chemical features, Fuel 324 (2022) 124617.

[7] N. Gaiser, T. Bierkandt, P. Oßwald, J. Zinsmeister, T. Kathrotia, S. Shaqiri, P. Hemberger, T. Kasper, M. Aigner, M. Köhler, Oxidation of oxymethylene ether (OME0-5): An experimental systematic study by mass spectrometry and photoelectron photoion coincidence spectroscopy, Fuel 313 (2022) 122650.

[8] Regulation (EU) 2024/1257 of the European Parliament and of the Council of 24 April 2024 on type-approval of motor vehicles and engines and of systems, components and separate technical units intended for such vehicles, with respect to their emissions and battery durability (Euro 7), Off. J. Eur. Union L 1257 (2024) ELI: http://data.europa.eu/eli/reg/2024/1257/oj.

[9] T. He, H.-y. Liu, Y. Wang, B. Wang, H. Liu, Z. Wang, Development of surrogate model for oxygenated wide-distillation fuel with polyoxymethylene dimethyl ether, SAE Int. J. Fuels Lubr. 10 (3) (2017) 803–814, Publisher: SAE International.

[10] F.H. Vermeire, H.-H. Carstensen, O. Herbinet, F. Battin-Leclerc, G.B. Marin, K.M. Van Geem, Experimental and modeling study of the pyrolysis and combustion of dimethoxymethane, Combust. Flame 190 (2018) 270–283.

[11] S. Jacobs, M. Döntgen, A.B. Alquaity, W.A. Kopp, L.C. Kröger, U. Burke, H. Pitsch, K. Leonhard, H.J. Curran, K.A. Heufer, Detailed kinetic modeling of dimethoxymethane. Part II: Experimental and theoretical study of the kinetics and reaction mechanism, Combust. Flame 205 (2019) 522–533.

[12] W. Sun, T. Tao, M. Lailliau, N. Hansen, B. Yang, P. Dagaut, Exploration of the oxidation chemistry of dimethoxymethane: Jet-stirred reactor experiments and kinetic modeling, Combust. Flame 193 (2018) 491–501.

[13] S. Ren, Z. Wang, B. Li, H. Liu, J. Wang, Development of a reduced poly-oxymethylene dimethyl ethers (PODEn) mechanism for engine applications, Fuel 238 (2019) 208–224.

[14] Q. Lin, K.L. Tay, D. Zhou, W. Yang, Development of a compact and robust Polyoxymethylene Dimethyl Ether 3 reaction mechanism for internal combustion engines, Energy Convers. Manage. 185 (2019) 35–43.

[15] B. Niu, M. Jia, Y. Chang, H. Duan, X. Dong, P. Wang, Construction of reduced oxidation mechanisms of polyoxymethylene dimethyl ethers (PODE1–6) with consistent structure using decoupling methodology and reaction rate rule, Combust. Flame 232 (2021) 111534.

[16] H. Wang, Z. Yao, X. Zhong, Q. Zuo, Z. Zheng, Y. Chen, M. Yao, Experimental and kinetic modeling studies on low-temperature oxidation of Polyoxymethylene Dimethyl Ether (DMM1-3) in a jet-stirred reactor, Combust. Flame 245 (2022) 112332.

[17] T. He, Z. Wang, X. You, H. Liu, Y. Wang, X. Li, X. He, A chemical kinetic mechanism for the low- and intermediate-temperature combustion of Polyoxymethylene Dimethyl Ether 3 (PODE3), Fuel 212 (2018) 223–235.

[18] L. Cai, S. Jacobs, R. Langer, F. Vom Lehn, K.A. Heufer, H. Pitsch, Auto-ignition of oxymethylene ethers (OMEn, n=2–4) as promising synthetic e-fuels from renewable electricity: shock tube experiments and automatic mechanism generation, Fuel 264 (2020) 116711.

[19] L. Cai, H. Pitsch, Mechanism optimization based on reaction rate rules, Combust. Flame 161 (2) (2014) 405–415.

[20] K. De Ras, M. Kusenberg, G. Vanhove, Y. Fenard, A. Eschenbacher, R.J. Varghese, J. Aerssens, R. Van De Vijver, L.-S. Tran, J.W. Thybaut, K.M. Van Geem, A detailed experimental and kinetic modeling study on pyrolysis and oxidation of oxymethylene ether-2 (OME-2), Combust. Flame 238 (2022) 111914.

[21] K. De Ras, M. Kusenberg, J.W. Thybaut, K.M. Van Geem, Unraveling the carbene chemistry of oxymethylene ethers: Experimental investigation and kinetic modeling of the high-temperature pyrolysis of OME-2, Proc. Combust. Inst. 39 (1) (2023) 125–133.

[22] K.P. Shrestha, S. Eckart, S. Drost, C. Fritsche, R. Schießl, L. Seidel, U. Maas, H. Krause, F. Mauss, A comprehensive kinetic modeling of oxymethylene ethers (OMEn, n=1–3) oxidation - laminar flame speed and ignition delay time measurements, Combust. Flame 246 (2022) 112426.

[23] T. Kathrotia, P. Oßwald, C. Naumann, S. Richter, M. Köhler, Combustion kinetics of alternative jet fuels, ßpart-II: Reaction model for fuel surrogate, Fuel 302 (2021) 120736.

[24] E. Ranzi, A. Frassoldati, S. Granata, T. Faravelli, Wide-range kinetic modeling study of the pyrolysis, partial oxidation, and combustion of heavy *n* -alkanes, Ind. Eng. Chem. Res. 44 (14) (2005) 5170–5183.

[25] G. Bagheri, E. Ranzi, M. Pelucchi, A. Parente, A. Frassoldati, T. Faravelli, Comprehensive kinetic study of combustion technologies for low environmental impact: MILD and OXY-fuel combustion of methane, Combust. Flame 212 (2020) 142–155.

[26] U. Burke, K.P. Somers, P. O'Toole, C.M. Zinner, N. Marquet, G. Bourque, E.L. Petersen, W.K. Metcalfe, Z. Serinyel, H.J. Curran, An ignition delay and kinetic modeling study of methane, dimethyl ether, and their mixtures at high pressures, Combust. Flame 162 (2) (2015) 315–330.

[27] A. Stagni, S. Schmitt, M. Pelucchi, A. Frassoldati, K. Kohse-Höinghaus, T. Faravelli, Dimethyl ether oxidation analyzed in a given flow reactor: Experimental and modeling uncertainties, Combust. Flame 240 (2022) 111998.

[28] A. Pegurri, T. Dinelli, L. Pratali Maffei, T. Faravelli, A. Stagni, Coupling chemical lumping to data-driven optimization for the kinetic modeling of dimethoxymethane (DMM) combustion, Combust. Flame 260 (2024) 113202.

[29] M. Pelucchi, S. Namysl, E. Ranzi, A. Rodriguez, C. Rizzo, K.P. Somers, Y. Zhang, O. Herbinet, H.J. Curran, F. Battin-Leclerc, T. Faravelli, Combustion of n-C3–C6 linear alcohols: An experimental and kinetic modeling study. Part I: Reaction classes, rate rules, model lumping, and validation, Energy Fuels 34 (11) (2020) 14688–14707, Publisher: American Chemical Society.

[30] E. Ranzi, M. Dente, A. Goldaniga, G. Bozzano, T. Faravelli, Lumping procedures in detailed kinetic modeling of gasification, pyrolysis, partial oxidation and combustion of hydrocarbon mixtures, Prog. Energy Combust. Sci. 27 (1) (2001) 99–139.

[31] M. Fürst, A. Bertolino, A. Cuoci, T. Faravelli, A. Frassoldati, A. Parente, OptiSMOKE++: A toolbox for optimization of chemical kinetic mechanisms, Comput. Phys. Comm. 264 (2021) 107940.

[32] A. Bertolino, M. Fürst, A. Stagni, A. Frassoldati, M. Pelucchi, C. Cavallotti, T. Faravelli, A. Parente, An evolutionary, data-driven approach for mechanism optimization: theory and application to ammonia combustion, Combust. Flame 229 (2021) 111366.

[33] A. Cuoci, A. Frassoldati, T. Faravelli, E. Ranzi, OpenSMOKE++: An object-oriented framework for the numerical modeling of reactive systems with detailed kinetic mechanisms, Comput. Phys. Comm. 192 (2015) 237–264.

[34] M. Pelucchi, A. Stagni, T. Faravelli, Chapter 15 - Addressing the complexity of combustion kinetics: Data management and automatic model validation, in: T. Faravelli, F. Manenti, E. Ranzi (Eds.), in: Computer Aided Chemical Engineering, vol. 45, Elsevier, 2019, pp. 763–798.

[35] M. Bernardi, M. Pelucchi, A. Stagni, L. Sangalli, A. Cuoci, A. Frassoldati, P. Secchi, T. Faravelli, Curve matching, a generalized framework for models/experiments comparison: An application to n-heptane combustion kinetic mechanisms, Combust. Flame 168 (2016) 186–203.

[36] X. Zhong, H. Wang, Q. Zuo, Z. Zheng, J. Wang, W. Yin, M. Yao, Experimental and kinetic modeling studies of polyoxymethylene dimethyl ether (PODE) pyrolysis in jet stirred reactor, J. Anal. Appl. Pyrol. 159 (2021) 105332.

[37] E. Ramalli, T. Dinelli, A. Nobili, A. Stagni, B. Pernici, T. Faravelli, Automatic validation and analysis of predictive models by means of big data and data science, Chem. Eng. J. 454 (2023) 140149.

[38] T. Dinelli, L. Pratali Maffei, A. Pegurri, A. Puri, A. Stagni, T. Faravelli, Automated kinetic mechanism evaluation for e-fuels using SciExpeM: The case of oxymethylene ethers, Capri, Italy, 2023, pp. 2023–24–0092.

[39] E. Ranzi, A. Frassoldati, R. Grana, A. Cuoci, T. Faravelli, A.P. Kelley, C.K. Law, Hierarchical and comparative kinetic modeling of laminar flame speeds of hydrocarbon and oxygenated fuels, Prog. Energy Combust. Sci. 38 (4) (2012) 468–501.

[40] Q. Wang, W. Sun, L. Guo, S. Lin, P. Cheng, H. Zhang, Y. Yan, Experimental and kinetic study on the laminar burning speed, Markstein length and cellular instability of oxygenated fuels, Fuel 297 (2021) 120754.